Facultad de Ciencias Naturales y Exactas
Universidad del Valle

The use of Entanglement Entropy to Classify Quantum Phase Transitions in 1D Ultracold Spinor Bosons

Karen Rodrìguez Ramìrez
Universidad Valle

Received: February, 17 2017 Accepted: February 28, 2017

Pag. 23-36.

Abstract

In this paper, we discuss a novel method based on a quantum-information-tool suitable to identify and characterize quantum-phases and phase transitions in a broad set of lattice models relevant in condensed-matter systems. The method relies on the entanglement entropy which, for instance, can be calculated using the Matrix Product State (MPS) algorithm, or any other method, for several system sizes to perform an appropriate scaling. Particularly, this advanced method has been applied for a finite 1D system of repulsively interacting spin-1 bosons and obtaining the universality class via the calculation of the central charge for the external field-induced phase transition between the dimerized phase and the XY-nematic phase in the antiferromagnetic regime. Finally, we briefly discuss how this method has been recently used to identify topological phases.

Keywords: entanglement entropy, ultracold atoms, spinor bosons, optical lattice.
Doi: http://dx.doi.org/10.25100/rc.v21i1.6342

1 Introduction

Ultracold gases is a multidisciplinary field, which lies in the intersection of several physics fields such as quantum information, condensed matter, quantum mechanics, non-linear physics, and statistical mechanics with a very strong contribution of numerical methods. Ultracold gases in optical lattices constitute an extraordinary tool for the analysis of strongly correlated gases under extremely well controlled conditions [1, 2], as highlighted by the observation of the superfluid to Mott-insulator (MI) transition in ultracold bosons [3], recently followed by the realization of the metal to MI transition in two-component fermions [4, 5].

The optical lattice potential is constructed using counter propagating laser beams. These are able to trap the atoms which are already at ultralow temperatures. The most interesting feature of this kind of systems is the tunability of the interactions, making the field very promising because of its high controllability. The perfect periodic optical potential resembles the electron moving in a periodic array of ions which develops a band structure. In the present work we concentrate on the physics of the lowest energy band. In the present work we concentrate on the physics of the lowest energy band.

In 1937, it was pointed out that a variety of transition metal oxides predicted to be conductors by band theory were actually insulators [6]. About the same time, Nevill Mott and Rudolf Peierls predicted that the failure in the theoretical description can be solved by including the interactions between electrons [7]. But it was until 1963 when Jhon Hubbard presented the simplest model for interacting electrons in a periodic potential, the nowadays called Hubbard model [8]. This model takes into account the kinetic energy of the particles given by a hopping term and an interacting contact potential given by,

$$V\left(\vec{r}-\vec{r}'\right)=g\delta\left(\vec{r}-\vec{r}'\right), \tag{1}$$

where $g = 4\pi\ \hbar^2 a/m_a$ is the interaction strength. This is an isotropic pseudo-potential determined by the particle s-wave scattering length a for the alkali-like atoms and m_a is the atomic mass. Having the periodic potential one can loaded it up with fermions, bosons, spins, molecules, etc. The initial atomic cloud is in the degenerate regime and exhibits all its quantum mechanical behavior. This regime for bosons is the socalled Bose-Einstein Condensation and is achieved when the De Bloglie thermal wavefunction, $\lambda_T = \sqrt{2\pi\hbar^2/(kBmaT)}$, is larger than the interparticle distance and therefore all the particles go to the lowest energy state exhibiting a giant matter-wave. For fermions, due to the Pauli exclusion principle, the fermionic cloud in this regime is broader than the bosonic cloud making the experimental realization harder but not impossible [4,5].

It is important to emphasize how the achievement of these low temperatures had generated a boost in the experimental and theoretical techniques with such impact that the pioneers were already awarded with the Nobel Prize. In 1997, S. Chu, Cohen-Tannoudji and W. D. Phillips were awarded for the development of methods to cool and trap atoms with laser light". In 2001, E. A. Cornell, W. Ketterle and C. E. Wieman were awarded for the achievement of Bose-Einstein condensation in dilute gases of alkali atoms and for early fundamental studies of the properties of the condensates". And very recently, in 2012, S. Haroche and D. J. Wineland were awarded for ground-breaking experimental methods that enable measuring and manipulation of individual quantum systems".

Optical traps permit the simultaneous trapping of various Zeeman sublevels, allowing for multicomponent (spinor) gases. Spinor bosons have attracted a large interest due to their internal degrees of freedom since it gives rise to rich ground-state physics and spinor dynamics [9-12]. Spinor gases in lattices are particularly exciting, since they provide unique possibilities for the analysis of quantum magnetism.

Spin-1 gases are the simplest spinor system beyond the two-component isospin-1=2. Depending on inter-particle interactions [9, 10], (given by the *s*-wave scattering lengths $a_{0,2}$ for collisions with total spin 0 and 2), spin-1 BECs present a ferromagnetic (FM) ground state (for $a_0 > a_2$, as in ^{87}Rb F = 1 [12]) or an antiferromagnetic (AFM) one (for $a_2 > a_0$, as in ^{23}Na [11]), also called polar. The case $a_0 = a_2$ exhibits an enlarged SU(3) symmetry with a highly degenerate ground state [13].

The spinor system exhibits two interaction channels (given by the allowed total spins) and two collision types. Being m_i the z-component of the particle i, there is a spin preserving collision ($m_1 + m_2 = m_1 + m_2$) where income and outcome spins have the same projections and the most interesting spin changing collision ($m_1 + m_2 = m_3 + m_4$) where outcome differs from income spins, but always conserves the spin z-projection.

Most spin-1 species are naturally close to the SU(3) point ($a_0 \approx a_2$). But small external perturbations as Zeeman shifts may have a large effect, reducing the system symmetry and thus, favoring different phases. Since interactions preserve the magnetization M, the linear Zeeman effect may be gauged out (although the phase diagram depends on M [14, 15]). On the contrary, the quadratic Zeeman effect (QZE) plays a crucial role in spinor gases. In spite of its importance, the role of the QZE in the quantum phases of spin-1 lattice bosons remains to a large extent unexplored. We note that the QZE may be controlled by means of microwave and optical techniques [16, 17]. There is a 3d mean field analysis [15], where it was shown that for finite M the QZE may lead to nematic-to-ferromagnetic (or partially magnetic) transitions and a complete phase diagram for the Mott-insulator phases of spin-1 bosons in the presence of QZE is presented in Ref. [18], where several techniques such as effective field theory (for any dimension), matrix product state (MPS) algorithm [19], (i.e. density matrix renormalization group (DMRG) [20]) and Lanczos diagonalization have been combined to obtain the phase boundaries and the characterization of the phase transitions. In addition, optical Feshbach resonances [21, 22], permit the modification of the ratio a_2/a_0, so that the full phase diagram may be explored with current techniques.

Recently, the interest on quantum entanglement in several communities has been growing [23]. This is due to the fact that in a pure bipartite state, having measured only part of the system (a subsystem), it is possible to have information of the whole quantum state if there is entanglement among the parts [24]. In fact, the corresponding von Neumann entropy associated to the reduced density matrix provides the

entanglement entropy of the measured subsystem. Nowadays, it becomes a key tool in the many-body strongly-correlated quantum systems analysis reveling nonlocal information and therefore a suitable mechanism to study quantum phases and phase transitions [25, 26].

2 Spin-1 Lattice Bosons

In the more general case for a balance bosonic mixture, the system is described by the Bose-Hubbard-like Hamiltonian given by:

$$\hat{H} - \mu\hat{N} = -t \sum_{<i,j>,m} \left\{ \hat{\Psi}^{\dagger}_{m,i} \hat{\Psi}_{m,j} + \text{h.c.} \right\} - \mu \sum_{i,m} \hat{n}_{m,i} + \sum_{i,\vec{m}} V_{1,2,3,4} \hat{\Psi}^{\dagger}_{m_1,i} \hat{\Psi}^{\dagger}_{m_2,i} \hat{\Psi}^{\dagger}_{m_3,i} \hat{\Psi}^{\dagger}_{m_4,i} + \sum_{i} q \left(\hat{S}^{z}_{i} \right)^2 . \quad (2)$$

Here, the spinor operator is a three-component vector $\hat{\Psi}^T = (\hat{\Psi}_{-1}, \hat{\Psi}_0, \hat{\Psi}_1)$ involving three m_F states. Aditionaly, μ is the chemical potential, which is the energy needed to add to or extract a particle from the system. The hopping strength t measures the kinetic energy of the particles and the sum is performed over all nearest neighbors $< i, j >$, allowing the generalization to any dimension. $V_{1,2,3,4}$ is the on-site interaction and the last term accounts for the quadratic Zeeman effect or single ion anisotropy as it is called in the condensed matter community. At low-energy, only *s*-wave scattering is relevant and the interaction takes the already mentioned contact form:

$$\mathrm{V}\left(\vec{r}_1 - \vec{r}_2\right) = \delta\left(\vec{r}_1 - \vec{r}_2\right) \sum_{F} g_F \hat{P}_F . \quad (3)$$

Hence, the on-site interaction is expressed in terms of two interacting channels using the projector operators $\hat{P}\mathrm{F} = \sum_{mF=}^{-F}{}_{\text{-F}} |F, m_f\rangle \langle \mathrm{F}, m_F|$ in each of the allowed total spins, $F = F_1 + F_2 = 0, 2$.

$$\hat{H}_{\mathrm{V}} = g_0 \sum_{i} \hat{P}^{\dagger}_{00,\mathrm{i}} \hat{P}^{\dagger}_{00,\mathrm{i}} + g \sum_{m_F,i} \hat{P}^{\dagger}_{2\mathrm{m}_F,\mathrm{i}} \hat{P}^{\dagger}_{2\mathrm{m}_F,\mathrm{i}} . \quad (4)$$

The Bose-Hubbard Hamiltonian exhibits two distinctive phases, the Mottinsulator or commensurate phase and the superfluid or incommensurable phase. We consider repulsively interacting ultracold spin-1 bosons in a *d*-dimensional hypercubic lattice, prepared in a balanced mixture (M = 0). In free space, the inter-particle interactions are characterized by the coupling constants $g_{0,2} = 4\pi\hbar^2 a_{0,2}/m_a$. In the presence of a lattice the onsite energies $\tilde{g}_{0,2}$ are proportional to $g_{0,2}$ and depend as well on lattice parameters [27]. At integer filling, the system enters in the MI regime if the (positive) on-site energies are much larger than the hopping parameter, $\tilde{g}_{0,2} \gg t$. Performing quasi-degenerate second-order perturbation theory in t using the standard Van Vleck transformation [28], the low-energy physics is achieved by means of superexchange processes, being described by an effective bilinear-biquadratic Hamiltonian spin [27, 29]:

$$\hat{H} = -\sum_{\langle i,j \rangle} \left[J_1 \mathrm{S}_i \cdot \mathrm{S}_j + J_2 \left(\mathrm{S}_i \cdot \mathrm{S}_i \right)^2 \right] - DJ \sum_i \left(S_i^z \right)^2, \tag{5}$$

where S_i are spin-1 operators at site i, the sum runs over nearest neighbors, and the coefficients are given by:

$$J_1 = \frac{2t^2}{\tilde{g}_2}, \quad \text{and} \quad J_2 = \frac{2t^2}{3\tilde{g}_2} + \frac{4t^2}{3\tilde{g}_0}, \tag{6}$$

being both positive quantities. The FM case ($a_0 > a_2$ as discussed before) corresponds to $J_1 > J_2$, whereas the AFM case ($a_2 > a_0$) results in $J_2 > J_1$. Typically, $a_0 \approx a_2$, which corresponds to the vicinity of the SU(3) point ($J_1 \approx J_2$). The last term in Eq. (2) describes the QZE that is characterized by the externally controllable constant $q = DJ$ and plays a crucial role in the system. In the following, a standard parameter has been used:

$$J_1 = -J \cos(\theta), \quad \text{and} \quad J_2 = -J \sin(\theta), \tag{7}$$

where θ lies in the interval ($-\pi + \arctan \frac{1}{3}$, $-\frac{\pi}{2}$) as the ratio g_2/g_0 goes from 0 to $+\infty$ and uses $J = \sqrt{J^2{}_1 + J^2{}_2}$ as the energy unit ($J = 1$).

This document also points out how a controlled tuning of the QZE may permit the observation of field-induced phase transitions in spin-1 lattice bosons, which are precluded by the simple use of the linear Zeeman effect due to conservation of M and thus, are absent in spin-1/2 systems.

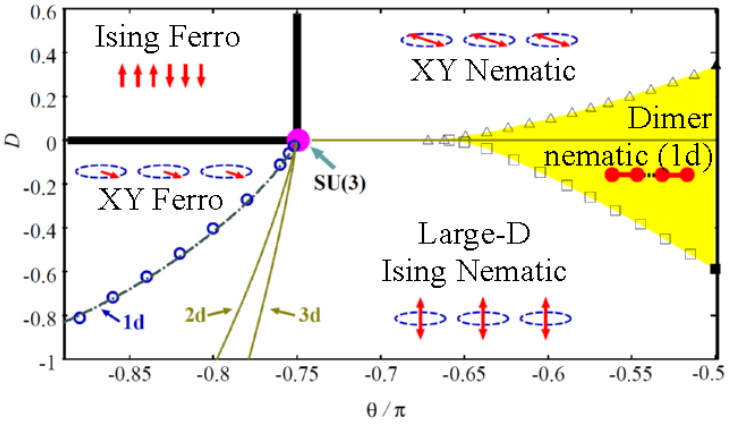

Figure 1: Phases of the spin-1 chain bosons, as a function of θ and the QZE parameter D. Solid bold lines correspond to first order phase transitions for any dimension d. Symbols represent numerical data for $d = 1$. Kosterlitz-Thouless transition line in the FM side (circles), and in the AFM side: the Kosterlitz-Thouless transition for D_c^+ (triangles) and the Ising-like transition for D_c^- (squares) are the limits of the dimerized phase, filled region only in 1d. The XY-FM to large-D transition lines retrieved from the field-theory are represented by dashed line for 1d, and the solid lines correspond to 2d and 3d as it is shown.

Spin-1 lattice bosons have attracted a strong interest, for which a wealth of quantum phases have been predicted (see Ref. [18] and references within). The phase diagram of repulsively interacting spin-1 bosons in optical lattices at unit filling in the presence of an externally induced quadratic Zeeman field obtained in Ref. [18] is shown in Figure 1. The phase diagram was obtained using the MPS method with open boundary conditions, for up to 42 sites and matrix dimension 30 correspondingly[1]. For ferromagnetic interactions and negative values of D, the phase transition line between the XY-ferromagnetic and large-D phases has been done by means of the fidelity susceptibility [30]. The studies show that a leading finite size extrapolation of 1=L2 law [31] (including the cases when logarithmic correction are present [32] confirms that the transition is Kosterlitz-Thouless kind [33] For antiferromagnetic interactions, in 2d and 3d the MI states at odd filling are nematic [27, 34], whereas in 1d quantum fluctuations lead to spontaneous dimerization [27, 35-40].

In the presence of an external field, the critical field curves $D_c^{\pm}$ have been retrieved using Lanczos diagonalizing for periodic systems of up to $L = 16$ sites and restricting the calculations to the different magnetization manifolds to reduce the Hilbert space dimension. In the Figure 1, the D_c^{+} curve (triangles) represents the transition between the dimerized and the XY-nematic phases. Its finite size extrapolation follows a $1=L^2$ law, confirming the Kosterlitz-Thouless nature with central charge $c = 1$. The D_c^{-} curve (squares) shows the transition between dimerized and large-D phases. We performed the calculations by means of the MPS method and found that this is an Ising-like transition since its central charge is $c = 0.5$ as it is discussed in detail in the subsection 3.1. When approaching the SU(3) point, the numerical simulations cannot recover the exponentially small dimerized region, which basically reduces to the $D = 0$ line.

3 Entanglement Entropy

Based on the fact that several numerical implementations lead to pure states, we restrict the discussion to pure entangled states. The aim of the present document is to discuss the entanglement entropy as a novel tool, useful to characterize phases and phase transitions in a broad set of lattice models relevant for condensed matter systems, which is the entanglement entropy.

Figure 2: A bipartite spin-chain divided in two subsystems such as a block (B) and an environment (E).

[1] Due to the 1D character of the physical system, the Hilbert space grows logarithmically, hence, the MPS matrix dimension does not explode, which is actually the advantage of the method. Particularly, at the vicinity of critical points the possibility to reach local minima, instead of the global one or ground state, is actually a problem and makes longer the calculation times. The matrix dimension is obtained in a standard fashion by increasing it while a local and/or global observable are tracked, such as density and/or energy, once the physical properties are invariant of the matrix dimension, the minimum size is chosen.

A bipartite pure quantum state described by $|\Psi\rangle$, consisting of two subsystems a block (B) and an environment (E) as depicted in the Figure 2, is generally expressed as $|\Psi\rangle = \sum_{ij} a_{ij} |B_i\rangle \otimes |E_j\rangle$, where $\{|B_i\rangle\}$and $\{|E_i\rangle\}$ are the complete set of orthonormal basis vectors in heir respective Hilbert subspaces. The tensor product state contains $N_B N_E$ expansion coefficients and could be very difficult to manipulate. Here, N_B (N_E) is the dimension of the ubspace B(E).

We consider physical lattice systems made of an array with L lattice sites. Let us separate the bipartite (two-subsystem) system applying the Schmidt decomposition (SD) [41]. Following this decomposition, any arbitrary pure state of a bipartite system can be written as

$$\left|\Psi\right\rangle = \sum_{\alpha_L=1}^{N_B} \lambda_\alpha \left|\alpha_B\right\rangle \otimes \left|\alpha_E\right\rangle, \tag{8}$$

where $\{|\alpha_B\rangle\}$ (on the block) and $\{|\alpha_E\rangle\}$ (on the environment) are two orthonormal base sets belonging to the respective Hilbert subspaces, each with at most N_B base elements when $N_E > N_B$. The coefficients λ_α are non-negative real numbers satisfying $\sum \alpha L\ \lambda_\alpha^2 = 1$, known as Schmidt coefficients and α running in the reduced Hilbert subspace.

Let us recall that the density matrix operator for a pure state is written as $\hat{\rho} = |\Psi\rangle\langle\Psi|$, and the diagonalizing of $\hat{\rho}$ gives us $\hat{\rho}\ |\rho\alpha\rangle = \rho\alpha|\rho\alpha\rangle$. Interestingly, the mathematics-physics connection among the Schmidt coefficients and the density matrix eigenvalues is given by $\lambda_\alpha^2 = \rho_\alpha$.

In a pure state, there is only one density matrix eigenvalue. But the reduced density matrix for the system Block ρ^ B =∑α λ_α^2 ln|αB⟩⟨αB| represents a mixed state where the entanglement entropy can be measured using the Von Neumann entropy.

$$S = -\sum_\alpha \lambda_\alpha^2 \ln\left(\lambda_\alpha^2\right). \tag{9}$$

Let us point out that the entanglement entropy is used as a resource to diagnose new quantum phases and phase transitions in condensed matter systems [42]. Nevertheless, to perform a characterization of a quantum system, it is important to use several techniques to compare the behavior since different systems can present different responses to a single tool.

3.1 Central charge

For gapless or critical systems in one dimension, the quantum critical points can be described by 2d conformal field theories, there, the entanglement entropy diverges logarithmically, with the universal coefficient determined by the central charge. The latter is a measure of the number of degrees of freedom whose gap vanishes at the critical point [43-45]. Hence, the universality class of a phase transition can be determined by means of the central charge [46]. Interestingly, there exists nontrivial

systems with fractional central charge, as it is the case for the Ising model where c = 1/2.

In order to classify the phase transition lying between the dimerized phase and the Ising nematic (Figure 1), it is when $D = D_c^-$, the central charge at D = 0, θ = -0:73π was computed. This value lies in the region where the XY-nematic and large-D phases meet each other at D = 0. Strictly speaking, this point is inside the dimerized phase, but since the correlation length is extremely large, the system can be considered as gapless.

The block entanglement entropy for a finite 1d system of size L divided into two pieces of size l (block) and L - l (environment), Figure 2, in the context of the conformal field theory [47-49], behaves as:

$$S = \frac{c}{6}\log\left[\frac{L}{\pi}\sin\left(\frac{\pi l}{L}\right)\right] + A, \tag{10}$$

where c is the central charge and A is a non-universal constant. Setting $l = \frac{L}{2}$, following Ref. [50], and using MPS method to evaluate S for several L values, the central charge is obtained from the slope of the curve, as it is shown in Figure 3. This method had retrieved $c \simeq 1.5$. The $D = D_c^+$ Kosterlitz-Thouless line has c = 1. Subtracting this contribution, we get $c = \frac{1}{2}$ for the $D = D_c^-$ line, conforming its Ising nature.

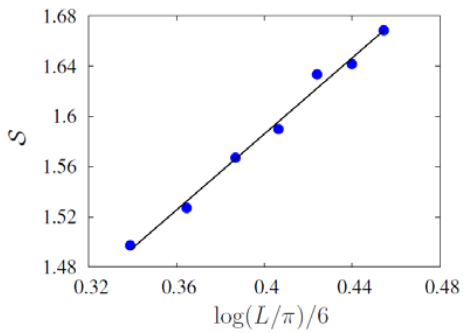

Figure 3: Central charge retrieved from the slope of the block entanglement entropy S. The calculation has been performed at θ = -0:73π for several system lengths. The fitting curve is given by $f(x)$ = 1:51508x + 0:980015 whose slope is c = 1:515 ± 0:065.

It is also interesting to quantify how much entanglement entropy occurs in the ground state of local and quasi-local Hamiltonians, in general, the measurement scales with L. If the entanglement between points is farther apart, some length scale ζ can be ignored. Then, the entanglement entropy should be determined by a shell of thickness ~ ζ around the block environment boundary (having the boundary a dimension of d - 1),

$$S \sim L^{d-1}\zeta \to S \sim L^{d-1} \quad \text{as} \quad L \to \infty, \tag{11}$$

with fixed system parameters. If there is no locality, any site in the block is likely to be entangled with a site in the environment as with another site in the block.

Hence, $S \sim L^d$. This relation is known as area law. This law has been established for 1d gapped systems [51] which are well approximated by MPS and can be simulated efficiently on a classical computer. Going beyond the area law [52] the entanglement scaling can also be used to distinguish conventional quantum critical points from non-Landau ones [53] and to diagnose critical phases in finite and infinite systems [54, 55],

$$\begin{aligned} S_n &= al - c_n + \ldots \quad \text{finite}, \\ S_n &= al - d_n \ln(l) + \ldots \text{infinite}, \end{aligned} \tag{12}$$

where S_n is the Renyi entropy [56] with a non-universal coefficient, and on the contrary c_n and d_n are universal n-dependent coefficients. In particular, the entanglement entropy $S = \lim_{n\to 1} S_n$ is well defined and universal [55].

The entanglement entropy is also useful to characterize topological phases by looking at the entanglement entropy spectrum. The later consists of the energies of the entanglement Hamiltonian block $\hat{H}_{EB} = -\ln \hat{\rho}_B$. In the topological phase, this spectrum is expected to be two fold degenerated [42, 57, 58]. These topological systems are unique states of matter that incorporate long-range quantum entanglement and host exotic excitations with fractional quantum statistics. The identification of topological phases in arbitrary realistic models has been reported by accurately calculating the topological entanglement entropy [59] using MPS. The argument is based on the fact that this algorithm systematically selects a minimally entangled state from the quasi-degenerated ground states.

4 Conclusions and outlook

In this work, we have reviewed the field-induced phase diagram of repulsively interacting spin-1 lattice bosons in the presence of the quadratic Zeeman field for both ferro and antiferromagnetic interactions, for the average filling of one boson per site.

In order to determine the nature and the precise location of the phase transitions, 1d numerical simulations must be performed. Particularly, we show the use of a novel and versatile technique based on the block entanglement entropy for 1d finite systems, to resolve the universality class of the spin Peierls and large-D transition by means of the central charge and performing finite size scaling.

The entanglement spectrum explodes also highly nonlocal properties offering the possibility of classifying 1d systems given its symmetry group [58]. Hence this technique, in principle, serves as a way to characterize from trivial to topological phases and phase transitions.

Acknowledgments. The author acknowledges the collaborators on the subject of spin-1-lattice bosons L. Santos, T. Vekua, A. K. Kolezhuk and A. Argüelles for fruitful work and discussions. This work has been supported by Universidad del Valle under the internal project CI 71072. K.R. acknowledges the support from CIBioFi, the Colombian Science, Technology and Innovation Fund (COLCIENCIAS: Francisco José de Caldas) under project 1106-712-49884 (contract No.264-2016), and the General Royalties System (CTeI-SGR Found), under contract No. BPIN 2013000100007.

References

1. Lewenstein M, Sanpera A, Ahufinger V, Damski B, Sen(De) A, Sen U. Ultracold atomic gases in optical lattices: mimicking condensed matter physics and beyond. Advanced Physics. 2007; 56(2): 243–379.

2. Bloch I, Dalibard J, Zwerger W. Many-body physics with ultracold gases. Rev Mod Phys. 2008; 80: 885.

3. Greiner M, Mandel O, Esslinger T, Hänsch TW, Bloch I. Collapse and revival of the matter wave field of a Bose–Einstein condensate. Nature. 2002; 415: 39-44.

4. Jördens R, Strohmaier N, Günter K, Moritz H, Esslinger T. A Mott insulator of fermionic atoms in an optical lattice. Nature. 2008; 455: 204-207.

5. Schneider U, Hackermuller L, Will S, Best Th, Bloch I, Costi TA. Metallic and insulating phases of repulsively interacting fermions in a 3D optical lattice. Science. 2008; 322 : 1520-1525.

6. de Boer JH, Verwey EJW. Semi-conductors with partially and with completely filled $_3d$-lattice bands. Proc Phys Soc. 1937; 49(4S): 59.

7. Mott NF, Peierls R. Discussion of the paper by de Boer and Verwey. Proc R Soc Lond A. 1963; 276: 238-257.

8. Hubbard J. Electron correlations in narrow energy bands. Proc Roy Soc Lond A. 1963; 276: 238-257.

9. Ho TL. Spinor bose condensates in optical traps. Phys Rev Lett. 1998; 81: 742-745.

10. Ohmi T, Machida K. Bose-Einstein condensation with internal degrees of freedom in alkali atom gases. J Phys Soc Jpn. 1998; 67: 1822–1825.

11. Stenger J, Inouye S, Stamper-Kurn DM, Miesner H-J, Chikkatur AP, Ketterle W. Spin domains in ground-state Bose–Einstein condensates. Nature. 1998; 396: 345-348.

12. Barrett MD, Sauer JA, Chapman MS. All-optical formation of an atomic Bose-Einstein condensate. Phys Rev Lett. 2001; 87: 010404.

13. Batista CD, Ortiz G, Gubernatis JE. Unveiling order behind complexity: coexistence of ferromagnetism and Bose-Einstein condensation. Phys Rev B. 2002; B65: 180402(R).

14. Imambekov A, Lukin M, Demler E. Magnetization plateaus for spin-one bosons in optical lattices: Stern-Gerlach experiments with strongly correlated atoms. Phys Rev Lett. 2004; 93(12): 120405.

15. Chung M-C, Yip S. Phase diagrams for spin-1 bosons in an optical lattice. Phys Rev A. 2009; A80(5): 053615.

16. Gerbier F, Widera A, Fölling S, Mandel O, Bloch I. Resonant control of spin dynamics in ultracold quantum gases by microwave dressing. Phys Rev A. 2006; A73: 041602(R).

17. Santos L, Fattori M, Stuhler J, Pfau T. Spinor condensates with a laser-induced quadratic Zeeman effect. Phys Rev A. 2007; A75(5): 053606.

18. Rodriguez, K. Argüelles A, Kolezhuk AK, Santos L, Vekua T. Field-induced phase transitions of repulsive spin-1 bosons in optical lattices. Phys Rev Lett. 2011;106(10): 105302.

19. Verstraete F, Garcia-Ripoll JJ, Cirac JI. Matrix product density operators: simulation of finite-temperature and dissipative systems. Phys Rev Lett. 2004; 93: 207204.

20. White SR, Noack RM. Real-space quantum renormalization groups. Phys Rev Lett. 1992; 68: 3487.

21. Fedichev PO, Kagan Y, Shlyapnikov GV, Walraven JTM. Influence of nearly resonant light on the scattering length in low-temperature atomic gases. Phys Rev Lett. 1996; 77: 2913.

22. Papoular DJ, Shlyapnikov GV, Dalibard J. Microwave-induced fano-feshbach resonances. Phys Rev A. 2010; A81: 041603(R).

23. He T, Magán JM, Vandoren S. Entanglement entropy of periodic sublattices. Phys Rev B. 2017; B95: 035130.

24. Calabrese P, Cardy J, Doyon B. Entanglement entropy in extended quantum systems. J Phys A: Math Theor. 2009; 42, 500301.

25. Mishmash RV, Motrunich OI. Entanglement entropy of composite fermi liquid states on the lattice: in support of the widom formula. Phys Rev B. 2016; B94(8): 081110(R).

26. Matsuura S, Wen X, Hung L-Y, Ryu S. Charged topological entanglement entropy. Phys Rev B. 2016; B93: 195113.

27. Imambekov A, Lukin M, Demler E. Spin-exchange interactions of spin-one bosons in optical lattices: singlet, nematic, and dimerized phases. Phys Rev A. 2003; A 68: 063602.

28. Van Vleck JH. On σ-Type doubling and electron spin in the spectra of diatomic molecules. Phys Rev. 1929; 33: 467.

29. Yip SK. Dimer state of spin-1 bosons in an optical lattice. Phys Rev Lett. 2003; 90: 250402.

30. You W-L, Li Y-W, Gu S-J. Fidelity, dynamic structure factor, and susceptibility in critical phenomena. Phys Rev E. 2007; E76, 022101.

31. Hsieh Y-D, Kao Y-J, Sandvik AW. Finite-size scaling method for the Berezinskii–Kosterlitz–Thouless transition. J Stat Mech. 2013; P09001.

32. Cardy JL. Operator content of two-dimensional conformally invariant theories. Nucl Phys B. 1986; B, 270: 186-204.

33. Haldane FDM. 'Luttinger liquid theory' of one-dimensional quantum fluids. I. Properties of the Luttinger model and their extension to the general 1D interacting spinless Fermi gas. J Phys C: Solid state Phys. 1981; 14(19): 2585.

34. Harada K, Kawashima N, Troyer M. Dimer-quadrupolar quantum phase transition in the quasi-one-dimensional Heisenberg model with biquadratic interaction. J Phys Soc Jpn. 2007; 76: 013703.

35. Zhou F, Snoek M. Spin singlet mott states and evidence for spin singlet quantum condensates of spin-one bosons in lattices. Ann Phys. 2003; 308: 692.

36. Demler E, Zhou F. Spinor bosonic atoms in optical lattices: symmetry breaking and Fractionalization. Phys Rev Lett. 2002; 88: 163001.

37. Rizzi M, Rossini D, De Chiara G, Montangero S, Fazio R. Phase diagram of spin-1 bosons on one-dimensional lattices. Phys Rev Lett. 2005; 95: 240404.

38. Chubukov AV. Fluctuations in spin nematics. J Phys Condens Matter 2. 1990; 2(6): 1593.

39. Chubukov AV. Spontaneous dimerization in quantum-spin chains. Phys Rev B. 1991; B43: 3337.

40. Fáth G, Sólyom J. Search for the nondimerized quantum nematic phase in the spin-1 chain. Phys Rev B. 1995; B51: 3620.

41. Schmidt E. Entwicklung willkurlicher funktionen nach systemen vorgeschriebener funktionen. Math Ann. 1907; 63: 433-476.

42. Stoudenmire EM, Alicea J, Starykh OA, Fisher MPA. Interaction effects in topological superconducting wires supporting Majorana fermions. Phys Rev B. 2011; 84: 014503.

43. Holzhey C, Larsen F, Wilczek F. Geometric and renormalized entropy in conformal field theory. Nucl Phys. 1994; B424: 443-467.

44. Vidal G, Latorre JI, Rico E, Kitaev A. Entanglement in quantum critical phenomena. Phys Rev Lett. 2003; 90: 227902.

45. Calabrese P, Cardy J. Entanglement entropy and quantum field theory: a non-technical introduction. Int J Quantum Infor. 2006; 4: 429.

46. Feiguin A, Trebst S, Ludwig AWW, Troyer M, Kitaev A, Wang Z, Freedman MH. Interacting anyons in topological quantum liquids: the golden chain. Phys Rev Lett. 2007; 98: 160409.

47. Affleck I. Universal term in the free energy at a critical point and the conformal anomaly. Phys Rev Lett. 1986; 56: 746.

48. Korepin VE. Universality of entropy scaling in one dimensional gapless models. Phys Rev Lett. 2004; 92: 096402.

49. Calabrese P, Cardy J. Entanglement entropy and quantum field theory. J Stat Mech. 2004; P06002.

50. Tagliacozzo L, de Oliveira TR, Iblisdir S, Latorre JI. Scaling of entanglement support for matrix product states. Phys Rev B. 2008; B78(2): 024410.

51. Eisert J, Cramer M, Plenio MB. *Colloquium*: Area laws for the entanglement entropy. Rev Mod Phys. 2010; 82: 277.

52. Casini H, Mazzitelli FD, Testé E. Area terms in entanglement entropy. Phys Rev. 2015; D 91(10): 104035.

53. Swingle B, Senthil T. Geometric proof of the equality between entanglement and edge spectra. Phys Rev B. 2012; B86: 155131.

54. Casini H, Huerta M. Universal terms for the entanglement entropy in 2 + 1 dimensions. Nucl Phys B. 2007; B 764(3): 183-201.

55. Metlitski MA, Fuertes CA, Sachdev S. Entanglement entropy in the *O*(*N*) model. Phys Rev. 2009; B80: 115122.

56. Rényi A. on measures of entropy and information. Proceedings of the fourth Berkeley symposium on mathematics statistics and probability I. Berkeley, CA. 1960; 547-561.

57. Turner AM, Pollmann F, Berg E. Topological phases of one-dimensional fermions: an entanglement point of view. Phys Rev B. 2011; B83: 075102.

58. Pollmann F, Turner AM, Berg E, Oshikawa M. Entanglement spectrum of a topological phase in one dimension. Phys Rev B. 2010; B81: 064439.

59. Jiang H-C, Wang Z, Balents L. Identifying topological order by entanglement entropy. Nat Phys. 2012; 8: 902–905.

Dirección del autor

Karen Rodríguez Ramírez
Departamento de Física, Universidad del Valle, Cali - Colombia
karem.c.rodriguez@correounivalle.edu.co